

Title	Enhancement of the critical temperature of the pnictide superconductor $\text{LaFeAsO}_{1-x}\text{F}_x$ studied via $^{75}\text{As}$ NMR under pressure
Author(s)	Nakano, Tatsuya; Fujiwara, Naoki; Tatsumi, Kenichiro; Okada, Hironari; Takahashi, Hiroki; Kamihara, Yoichi; Hirano, Masahiro; Hosono, Hideo
Citation	Physical Review B (2010), 81(10)
Issue Date	2010-3-22
URL	<a href="http://hdl.handle.net/2433/241784">http://hdl.handle.net/2433/241784</a>
Right	©2010 American Physical Society
Type	Journal Article
Textversion	publisher

# Enhancement of the critical temperature of the pnictide superconductor $\text{LaFeAsO}_{1-x}\text{F}_x$ studied via $^{75}\text{As}$ NMR under pressure

Tatsuya Nakano,<sup>1</sup> Naoki Fujiwara,<sup>1,\*</sup> Kenichiro Tatsumi,<sup>1</sup> Hironari Okada,<sup>2,3</sup> Hiroki Takahashi,<sup>2,3</sup> Yoichi Kamihara,<sup>3,4</sup> Masahiro Hirano,<sup>5,6</sup> and Hideo Hosono<sup>4,5,6</sup>

<sup>1</sup>Graduate School of Human and Environmental Studies, Kyoto University, Yoshida-Nihonmatsu-cyo, Sakyo-ku, Kyoto 606-8501, Japan

<sup>2</sup>Department of Physics, College of Humanities and Sciences, Nihon University, Sakurajosui, Setagaya-ku, Tokyo 156-8550, Japan

<sup>3</sup>TRIP, Japan Science and Technology Agency (JST), Sanban-cho bldg. 5, Sanban-cho, Chiyoda-ku, Tokyo 102-0075, Japan

<sup>4</sup>Materials and Structures Laboratory (MSL), Tokyo Institute of Technology, 4259 Nagatsuda, Midori-ku, Yokohama 226-8503, Japan

<sup>5</sup>ERATO-SORST, Japan Science and Technology Agency (JST), Sanban-cho bldg. 5, Sanban-cho, Chiyoda-ku, Tokyo 102-0075, Japan

<sup>6</sup>Frontier Research Center (FRC), Tokyo Institute of Technology, 4259 Nagatsuda, Midori-ku, Yokohama 226-8503, Japan

(Received 10 December 2009; revised manuscript received 27 January 2010; published 22 March 2010)

Nuclear-magnetic-resonance measurements of an iron (Fe)-based superconductor  $\text{LaFeAsO}_{1-x}\text{F}_x$  ( $x=0.08$  and  $0.14$ ) were performed at ambient pressure and under pressure. The relaxation rate  $1/T_1$  for the overdoped samples ( $x=0.14$ ) shows  $T$ -linear behavior just above  $T_c$ , and pressure application enhances  $1/T_1T$  similar to the behavior of  $T_c$ . This implies that  $1/T_1T=\text{constant}$  originates from the Korringa relation, and an increase in the density of states at the Fermi energy  $D(E_F)$  leads to the enhancement of  $T_c$ . In the underdoped samples ( $x=0.08$ ),  $1/T_1$  measured at ambient pressure also shows  $T$ -linear behavior in a wide temperature range above  $T_c$ . However,  $1/T_1T$  shows Curie-Weiss-type  $T$  dependence at 3.0 GPa accompanied by a small increase in  $T_c$ , suggesting that predominant low-frequency antiferromagnetic fluctuation is not important for development of superconductivity or remarkable enhancement of  $T_c$ . The qualitatively different features between underdoped and overdoped samples are systematically explained by a band calculation with hole and electron pockets.

DOI: [10.1103/PhysRevB.81.100510](https://doi.org/10.1103/PhysRevB.81.100510)

PACS number(s): 74.70.Xa, 74.25.Ha, 74.62.Fj, 76.60.-k

$\text{LaFeAsO}_{1-x}\text{F}_x$  is the highly important compound that stimulated tremendous research activity in Fe-based high- $T_c$  superconductors.<sup>1</sup> The compound exhibits several phases with F substitution, i.e., electron doping, on the temperature-concentration ( $T$ - $x$ ) phase diagram.<sup>1,2</sup> A spin-density-wave-type antiferromagnetic (AF) ordering of the parent compound  $\text{LaFeAsO}$  is suppressed by F substitution, and superconductivity appears after the AF phase vanishes.<sup>2-5</sup>  $T_c$  weakly depends on the doping level. The optimal doping level is around  $x=0.11$  at which  $T_c$  reaches 26 K. Similar phenomena also appear in a “122” system,  $(\text{K}_{1-x}\text{X}_x)\text{Fe}_2\text{As}_2$  ( $X=\text{Sr}$  or  $\text{Ba}$ ).<sup>6-9</sup>

The  $T$ - $x$  phase diagram is reminiscent of hole doping in high- $T_c$  cuprates. However, unlike the case of high- $T_c$  cuprates, it is unclear whether AF spin fluctuation plays an important role in raising  $T_c$ . In the case of  $\text{LaFeAsO}_{1-x}\text{F}_x$ ,  $T_c$  is sensitive to pressure ( $P$ ), and shows a clear dome-shaped pressure dependence on the  $T$ - $P$  phase diagram.<sup>10</sup> The highest  $T_c$  is realized by applying pressure to optimally doped samples ( $x\sim 0.11$ ) or heavily doped samples ( $x\sim 0.14$ ).  $T_c$  of 26 and 20 K for  $x=0.11$  and  $0.14$ , respectively, goes up to 43 K with application of a pressure of 4–5 GPa.<sup>10-12</sup> [Fig. 1(a)] However,  $T_c$  for lightly doped samples ( $x=0.05$ ) hardly goes beyond 30 K even under high pressure.<sup>11,12</sup> The suppression of  $T_c$  suggests that a superconducting state with a high  $T_c$  is realized apart from the antiferromagnetically ordered phase on the  $T$ - $x$  phase diagram. To investigate the origin of the  $T_c$  enhancement under pressure, and the relationship between the low-frequency AF spin fluctuation and superconductivity in this material, we performed  $^{75}\text{As}$  ( $I=3/2$ )-nuclear-magnetic-resonance (NMR) measure-

ments under high pressure of underdoped samples ( $x=0.08$ ) and overdoped samples ( $x=0.14$ ). To determine  $T_c$  and investigate the  $P$  dependence, we also measured resistivity at pressures below 2.6 GPa using a piston-cylinder-type pressure cell and resistance above 4 GPa using a diamond-anvil cell.

The resistance and resistivity for  $x=0.08$  are plotted in

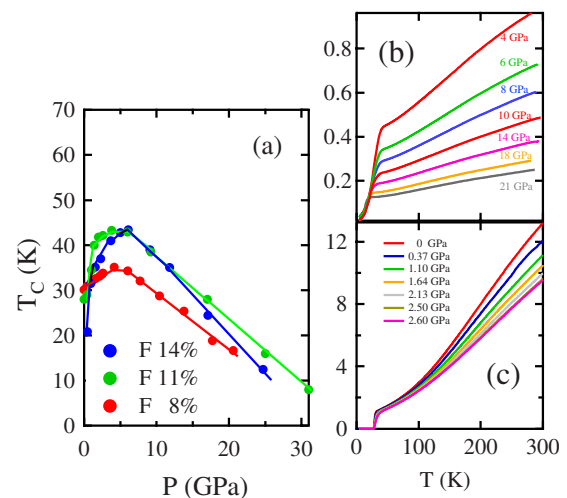


FIG. 1. (Color online) (a)  $P$  dependence of  $T_c$  measured using a piston-cylinder cell and a diamond-anvil cell. (b) Resistance for 8% doped samples at various pressures measured using a diamond-anvil cell. The unit of the vertical axis is ohm. (c) Resistivity for 8% doped samples at various pressures measured by using a piston-cylinder cell. The unit of the vertical axis is ohm centimeter.

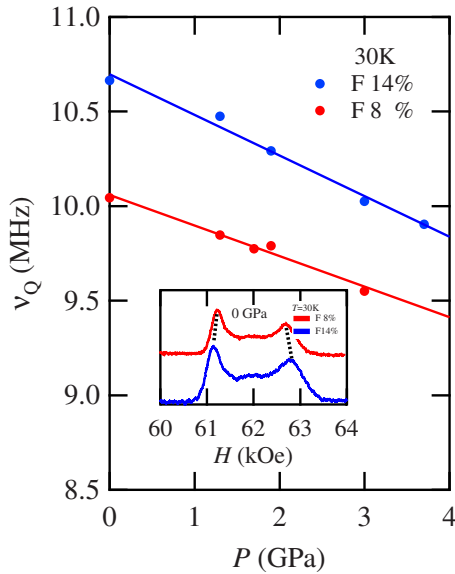


FIG. 2. (Color online)  $P$  dependence of pure quadrupole frequency of  $^{75}\text{As}$  nuclei. The inset shows field-swept spectra of the central transition,  $I=-1/2 \Leftrightarrow 1/2$ .

Figs. 1(b) and 1(c), respectively. The resistivity for  $x=0.14$  has been published elsewhere.<sup>11,12</sup> Their  $T_c$  values are determined by the onset of superconductivity. In both samples, zero resistivity was confirmed at low temperatures. The  $P$  dependence of  $T_c$  for  $x=0.08, 0.11$ , and  $0.14$  is plotted in Fig. 1(a).  $T_c$  for the underdoped regime ( $x < 0.11$ ) does not go beyond 35 K whereas that for the overdoped regime ( $x > 0.11$ ) exceeds 40 K.

We measured NMR spectra under pressure using randomly oriented powder samples. Field ( $H$ )-swept spectra of the central transition,  $I=-1/2 \Leftrightarrow 1/2$ , show a broad powder pattern, which prevented accurate Knight-shift measurements (Fig. 2 inset). The line shape is explained by considering the second-order quadrupole effect under a magnetic field.<sup>13</sup> The resonance position depends on the angle  $\theta$  between  $H$  and the maximum electric field gradient (EFG) at an As nucleus.<sup>13</sup> The lower- and higher-field peaks in the inset correspond to  $\theta=90^\circ$  and  $42^\circ$ , respectively. The separation between them is proportional to the square of the pure quadrupole frequency ( $\nu_Q$ ) except for a minor correction due to the asymmetry parameter ( $\eta$ ) of the EFG tensor.<sup>14</sup> We estimated  $\eta$  as 0.1 from the NMR spectra and found that  $\eta$  is insensitive to the doping level. The frequency  $\nu_Q$  is defined as  $2\nu_Q = eQV_{zz}/h$ , where  $Q$  and  $V_{zz}$  are the nuclear quadrupole moment and maximum EFG, respectively. The separation between the peaks decreases with increasing pressure. The results of  $\nu_Q$  at several pressures are plotted in the main panel of Fig. 2. The frequency  $\nu_Q$ , i.e.,  $V_{zz}$  originates from the on-site charge density and the surrounding Fe ions.  $V_{zz}$  is sensitive to the distance between Fe and As ions: a stretching of the Fe-As distance decreases EFG originating from the surrounding Fe ions and weakens the hybridization between As  $4p$  and Fe  $3d$  orbitals, which would lead to the decrease in the on-site charge density. The decrease in  $\nu_Q$  or EFG due to application of pressure can be explained by the stretching of the Fe-As distance. The stretching due to application of

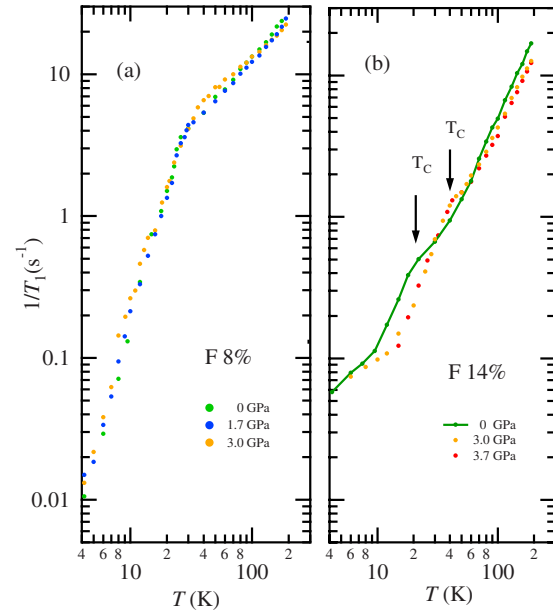


FIG. 3. (Color online)  $^{75}\text{As}$ -nuclear-magnetic-relaxation rate  $1/T_1$  for  $H \perp$  the maximum electric field gradient of  $^{75}\text{As}$ . (a) Underdoped regime ( $x=0.08$ ). (b) Overdoped regime ( $x=0.14$ ).

pressure has been observed from synchrotron-radiation measurements under high pressure.<sup>15</sup>

We measured the relaxation rate  $1/T_1$  at  $\theta=90^\circ$  using a saturation recovery method. The  $T$  dependence of  $1/T_1$  for  $x=0.08$  and  $0.14$  is shown in Figs. 3(a) and 3(b), respectively. The  $T$  dependence of  $1/T_1 T$  is shown in Fig. 4.  $1/T_1 T$  for the two doping levels shows qualitatively different  $T$  dependence.

In the case of  $x=0.14$ ,  $T$ -linear dependence is observed in a narrow  $T$  range just above  $T_c$ . The  $T$ -linear dependence is clearly observed as a plateau in Fig. 4.  $T_c$  values determined from the resistivity measurements are indicated by arrows in Figs. 3(b) and 4. The value of  $1/T_1 T$  is enhanced with increasing pressure similar to the behavior of  $T_c$ .  $1/T_1 T$  seems to change in accordance with  $T_c$  with increasing pressure: both  $1/T_1 T$  and  $T_c$  increase remarkably with increasing pressure from 0 to 3.0 GPa, and the change in  $1/T_1 T$  between 3.0

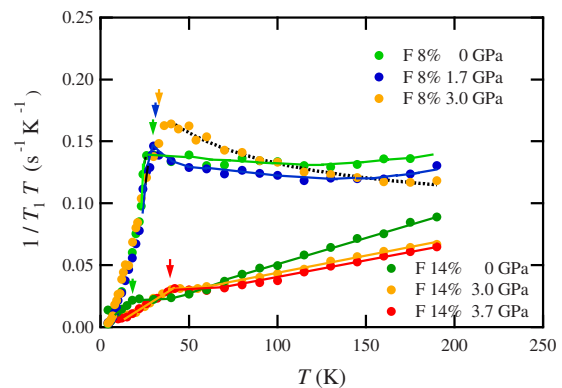


FIG. 4. (Color online)  $1/T_1 T$  measured at several pressures. The dotted curve represents a Curie-Weiss curve. The other lines are guide to the eyes.

and 3.7 GPa is small, similar to that in  $T_c$ . The  $T$ -linear dependence is attributable to the Korringa relation, and the value of  $1/T_1T$  just above  $T_c$  is proportional to the square of the density of states (DOS) at the Fermi energy,  $D(E_F)$ . At high temperatures, deviation from the  $T$ -linear dependence becomes remarkable. The increase in  $1/T_1T$  can be explained by a characteristic band structure of this system, as described below.<sup>16</sup> At low temperatures, another  $T$ -linear dependence appears, suggesting the existence of the impurity scatterings.<sup>17–19</sup> In the overdoped regime, the system can be well described as a band metal, and application of pressure causes an increase in  $D(E_F)$  and enhancement of  $T_c$ .

In the case of  $x=0.08$ ,  $1/T_1$  shows  $T$ -linear dependence in a wide  $T$  range above  $T_c$  at ambient pressure, and  $T^3$  dependence below  $T_c$ , as already reported by other groups.<sup>20–22</sup>  $T_c$  values determined from the resistivity measurements, indicated by arrows in Fig. 4, are consistent with those estimated from the change in  $1/T_1T$  within an accuracy of several kelvins. At first glance, the  $T$ -linear dependence is reminiscent of the Korringa relation, as in the case of  $x=0.14$ . However, it does not originate from the conventional Korringa relation: if the  $T$ -linear dependence originates from the Korringa relation, the estimated  $T_c$  should go beyond 40 K because the value of  $1/T_1T$ , namely,  $D(E_F)$  for  $x=0.08$  is much larger than that for  $x=0.14$ . Furthermore,  $1/T_1T \sim \text{constant}$ , observed at ambient pressure, breaks down under high pressure, as seen from the data at 3.0 GPa.  $1/T_1T$  increases monotonously toward  $T_c$ .  $1/T_1T$  at 1.7 GPa shows transitional behavior from  $1/T_1T \sim \text{constant}$  to Curie-Weiss behavior. The dotted curve in Fig. 4 represents a Curie-Weiss curve:  $1/T_1T = 0.09 + 6.2/(T+39)$  ( $\text{s}^{-1} \text{K}^{-1}$ ). The Curie-Weiss behavior is reminiscent of high- $T_c$  cuprates. Although low-frequency AF fluctuation predominates by applying pressure, an increase in  $T_c$  is small. Low-frequency AF fluctuation is not essential to achieving the highest  $T_c$ , although it would contribute to raising  $T_c$  to some extent: the highest  $T_c$  is realized for  $x=0.11–0.14$  without development of low-frequency AF fluctuation. It is concluded that low-frequency AF fluctuation suppresses the development of superconductivity or the enhancement of  $T_c$  in this material.

The qualitatively different features between samples with  $x=0.08$  and 0.14 are explained by a scenario based on a band calculation with electron and hole pockets.<sup>23,24</sup> The system can be treated as a simple two-dimensional square lattice of an Fe atom, although two Fe atoms are contained in the actual unit cell. In the unfolded Brillouin zone, hole pockets exist around  $\Gamma(0,0)$  and  $\Gamma'(\pi,\pi)$  in addition to electron pockets around M points.<sup>23</sup>  $\Gamma'(\pi,\pi)$  overlaps  $\Gamma(0,0)$  in the

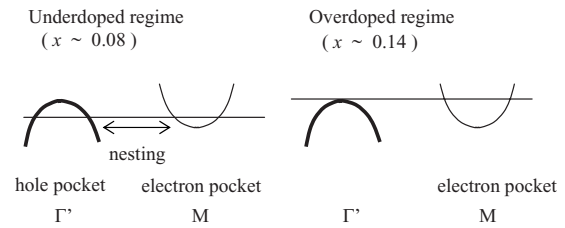


FIG. 5. A scheme of a two-band model. In the underdoped regime, nesting between hole and electron pockets causes AF fluctuation as seen in  $1/T_1T$  for the 8% doped samples at 3.0 GPa (Fig. 4). In the overdoped regime, the hole pockets around  $\Gamma'$  disappears and the system can be described as a band metal. The behavior is seen in  $1/T_1T$  for the 14% doped samples (Fig. 4).

original folded Brillouin zone. With increasing doping level, the Fermi energy moves upward and the hole pockets around  $\Gamma(\Gamma')$  become smaller. The hole pocket around  $\Gamma'(\pi,\pi)$  is sensitive to the doping level, and it first vanishes with increasing doping level, as illustrated in Fig. 5.<sup>25</sup> In the underdoped regime, the nesting between electron and hole pockets gives rise to AF fluctuation, which predominates and would suppress development of superconductivity, namely, remarkable enhancement of  $T_c$ . Application of pressure seems to promote the nesting. In the overdoped regime, the nesting becomes weak when electron doping moves the Fermi energy upward and the hole pockets around  $\Gamma(\Gamma')$  become smaller. In such a situation, remarkable enhancement of  $T_c$  is possible. When the hole pocket around  $\Gamma'$  vanishes, a large weight of DOS still remains just below the Fermi energy as illustrated in Fig. 5. The contribution from these energy levels presumably leads to an increase in  $1/T_1T$  at high temperatures, as seen in the  $x=0.14$  doped samples. The scenario can be expanded to other systems, such as hole-doped systems, in this case the Fermi energy moves downward with increasing doping level, and AF fluctuation predominates until the Fermi energy comes across the bottom of the electron band, which would suppress any rise in  $T_c$ . This scenario may answer the question of why the highest  $T_c$  (over 50 K) is realized only for “1111” systems. To investigate the origin of the highest  $T_c$  observed in a 1111 system, the pressure effect on the electron pockets around M seems important.

We would like to thank K. Kuroki and H. Ikeda for fruitful discussions and A. Hisada for experimental support. This work was partially supported by a Grant-in-Aid (KAKENHI 17340107) from the Ministry of Education, Science and Culture, Japan.

\*naoki@fujiwara.h.kyoto-u.ac.jp

<sup>1</sup>Y. Kamihara, T. Watanabe, M. Hirano, and H. Hosono, *J. Am. Chem. Soc.* **130**, 3296 (2008).

<sup>2</sup>H. Luetkens, H.-H. Klauss, M. Kraken, F. J. Litterst, T. Dellmann, R. Klingeler, C. Hess, R. Khasanov, A. Amato, C. Baines, M. Kosmala, O. J. Schumann, M. Braden, J. Hamann-Borrero, N. Leps, A. Kondrat, G. Behr, J. Werner, and B. Büchner, *Nature Mater.* **8**, 305 (2009).

<sup>3</sup>C. de la Cruz, Q. Huang, J. W. Lynn, J. Li, W. Ratcliff II, J. L. Zarestky, H. A. Mook, G. F. Chen, J. L. Luo, N. L. Wang, and P. Dai, *Nature (London)* **453**, 899 (2008).

<sup>4</sup>H.-H. Klauss, H. Luetkens, R. Klingeler, C. Hess, F. J. Litterst, M. Kraken, M. M. Korshunov, I. Eremin, S.-L. Drechsler, R. Khasanov, A. Amato, J. Hamann-Borrero, N. Leps, A. Kondrat,

- G. Behr, J. Werner, and B. Buchner, *Phys. Rev. Lett.* **101**, 077005 (2008).
- <sup>5</sup>Q. Huang, J. Zhao, J. W. Lynn, G. F. Chen, J. L. Luo, N. L. Wang, and P. Dai, *Phys. Rev. B* **78**, 054529 (2008).
- <sup>6</sup>K. Sasmal, B. Lv, B. Lorenz, A. M. Guloy, F. Chen, Y. Y. Xue, and C. W. Chu, *Phys. Rev. Lett.* **101**, 107007 (2008).
- <sup>7</sup>M. Rotter, M. Tegel, and D. Johrendt, *Phys. Rev. Lett.* **101**, 107006 (2008).
- <sup>8</sup>H. Chen, Y. Ren, Y. Qiu, W. Bao, R. H. Liu, G. Wu, T. Wu, Y. L. Xie, X. F. Wang, Q. Huang, and X. H. Chen, *EPL* **85**, 17006 (2009).
- <sup>9</sup>K. Igawa, H. Okada, H. Takahashi, S. Matsuishi, Y. Kamihara, M. Hirano, H. Hosono, K. Matsubayashi, and Y. Uwatoko, *J. Phys. Soc. Jpn.* **78**, 025001 (2009).
- <sup>10</sup>H. Takahashi, K. Igawa, K. Arii, Y. Kamihara, M. Hirano, and H. Hosono, *Nature (London)* **453**, 376 (2008).
- <sup>11</sup>H. Okada, K. Igawa, H. Takahashi, Y. Kamihara, M. Hirano, H. Hosono, K. Matsubayashi, and Y. Uwatoko, *J. Phys. Soc. Jpn.* **77**, 113712 (2008).
- <sup>12</sup>H. Takahashi, H. Okada, K. Igawa, K. Arii, Y. Kamihara, S. Matsuishi, M. Hirano, H. Hosono, K. Matsubayashi, and Y. Uwatoko, *J. Phys. Soc. Jpn.* **77** Suppl. C 78 (2008).
- <sup>13</sup>G. H. Stauss, *J. Chem. Phys.* **40**, 1988 (1964).
- <sup>14</sup>The asymmetry parameter  $\eta$  is defined as  $\eta = \frac{V_{xx} - V_{yy}}{V_{zz}}$ , where  $V_{zz}$ ,  $V_{xx}$ , and  $V_{yy}$  ( $|V_{xx}| \leq |V_{yy}|$ ) represent the maximum EFG and EFGs for the axes orthogonal to the principal axis  $z$ , respectively.
- <sup>15</sup>G. Garbarino, P. Toulemonde, M. Alvarez-Murga, A. Sow, M. Mezouar, and M. Nunez-Regueiro, *Phys. Rev. B* **78**, 100507(R) (2008).
- <sup>16</sup>H. Ikeda, *J. Phys. Soc. Jpn.* **77**, 123707 (2008).
- <sup>17</sup>K. Tatsumi, N. Fujiwara, H. Okada, H. Takahashi, Y. Kamihara, M. Hirano, and H. Hosono, *J. Phys. Soc. Jpn.* **78**, 023709 (2009).
- <sup>18</sup>D. Parker, O. V. Dolgov, M. M. Korshunov, A. A. Golubov, and I. I. Mazin, *Phys. Rev. B* **78**, 134524 (2008).
- <sup>19</sup>Y. Bang, H.-Y. Choi, and H. Won, *Phys. Rev. B* **79**, 054529 (2009).
- <sup>20</sup>Y. Nakai, K. Ishida, Y. Kamihara, M. Hirano, and H. Hosono, *J. Phys. Soc. Jpn.* **77**, 073701 (2008).
- <sup>21</sup>H.-J. Grafe, D. Paar, G. Lang, N. J. Curro, G. Behr, J. Werner, J. Hamann-Borrero, C. Hess, N. Leps, R. Klingeler, and B. Büchner, *Phys. Rev. Lett.* **101**, 047003 (2008).
- <sup>22</sup>S. Kawasaki, K. Shimada, G. F. Chen, J. L. Luo, N. L. Wang, and G.-q. Zheng, *Phys. Rev. B* **78**, 220506(R) (2008).
- <sup>23</sup>K. Kuroki, S. Onari, R. Arita, H. Usui, Y. Tanaka, H. Kontani, and H. Aoki, *Phys. Rev. Lett.* **101**, 087004 (2008).
- <sup>24</sup>I. I. Mazin, D. J. Singh, M. D. Johannes, and M. H. Du, *Phys. Rev. Lett.* **101**, 057003 (2008).
- <sup>25</sup>The hole pocket around  $\Gamma'$  vanishes at  $x=0.1$  (see Ref. 23) although both of hole pockets around  $\Gamma$  and  $\Gamma'$  exist for the undoped samples ( $x=0$ ) (see Ref. 16).